Received: 17 June 2021 | Revised: 12 September 2021 | Accepted: 12 October 2021

DOI: 10.1002/psp4.12733

ARTICLE

Physiologically-based pharmacokinetic modeling to evaluate in vitro-to-in vivo extrapolation for intestinal P-glycoprotein inhibition

Shinji Yamazaki[1] | **Raymond Evers**[2] | **Loeckie De Zwart**[3]

[1]Drug Metabolism & Pharmacokinetics, Janssen Research & Development, LLC, San Diego, California, USA

[2]Drug Metabolism & Pharmacokinetics, Janssen Research & Development, LLC, Spring House, Pennsylvania, USA

[3]Drug Metabolism & Pharmacokinetics, Janssen Research & Development, Beerse, Belgium

Correspondence
Shinji Yamazaki, Drug Metabolism & Pharmacokinetics, Janssen Research & Development, LLC, 3210 Merryfield Row, San Diego, CA 92121, USA.
Email: syamaza5@its.jnj.com

Funding information
This study was sponsored by Janssen Research & Development, LLC.

Abstract

As one of the key components in model-informed drug discovery and development, physiologically-based pharmacokinetic (PBPK) modeling linked with in vitro-to-in vivo extrapolation (IVIVE) is widely applied to quantitatively predict drug–drug interactions (DDIs) on drug-metabolizing enzymes and transporters. This study aimed to investigate an IVIVE for intestinal P-glycoprotein (Pgp, ABCB1)-mediated DDIs among three Pgp substrates, digoxin, dabigatran etexilate, and quinidine, and two Pgp inhibitors, itraconazole and verapamil, via PBPK modeling. For Pgp substrates, assuming unbound Michaelis-Menten constant (K_m) to be intrinsic, in vitro-to-in vivo scaling factors for maximal Pgp-mediated efflux rate (J_{max}) were optimized based on the clinically observed results without co-administration of Pgp inhibitors. For Pgp inhibitors, PBPK models utilized the reported in vitro values of Pgp inhibition constants (K_i), 1.0 μM for itraconazole and 2.0 μM for verapamil. Overall, the PBPK modeling sufficiently described Pgp-mediated DDIs between these substrates and inhibitors with the prediction errors of less than or equal to ±25% in most cases, suggesting a reasonable IVIVE for Pgp kinetics in the clinical DDI results. The modeling results also suggest that Pgp kinetic parameters of both the substrates (K_m and J_{max}) and the inhibitors (K_i) are sensitive to Pgp-mediated DDIs, thus being key for successful DDI prediction. It would also be critical to incorporate appropriate unbound inhibitor concentrations at the site of action into PBPK models. The present results support a quantitative prediction of Pgp-mediated DDIs using in vitro parameters, which will significantly increase the value of in vitro studies to design and run clinical DDI studies safely and effectively.

Study Highlights

WHAT IS THE CURRENT KNOWLEDGE ON THE TOPIC?

Physiologically-based pharmacokinetic (PBPK) modeling is increasingly being applied to predict transporter-mediated drug–drug interactions (DDIs); however,

there are currently knowledge gaps that limit the confidence of DDI predictions for modeling transporter kinetics of both substrates and inhibitors.

WHAT QUESTION DID THIS STUDY ADDRESS?

The aim of this study was to quantitatively investigate an in vitro-to-in vivo extrapolation (IVIVE) for intestinal Pgp-DDIs between three Pgp substrates, digoxin, dabigatran etexilate, and quinidine, and two Pgp inhibitors, itraconazole and verapamil. The PBPK-IVIVE approach utilized Pgp kinetic parameters determined in vitro such as unbound Michaelis-Menten constants and maximal efflux rates for the substrates and inhibition constants for the inhibitors.

WHAT DOES THIS STUDY ADD TO OUR KNOWLEDGE?

The present PBPK-IVIVE approach reasonably described clinically observed Pgp-DDI results, suggesting a consistent IVIVE for Pgp kinetics. The present modeling approach can be applicable to predict Pgp-DDIs with other Pgp substrates and inhibitors.

HOW MIGHT THIS CHANGE DRUG DISCOVERY, DEVELOPMENT, AND/OR THERAPEUTICS?

The present PBPK-IVIVE results support a quantitative Pgp-DDI prediction using in vitro Pgp kinetic parameters, thus presenting advancement toward quantitative Pgp-DDI prediction in clinical studies and/or case scenarios that have not been tested clinically yet.

INTRODUCTION

Model-informed drug discovery and development (MID3) has become an important framework to quantitatively maximize the benefit-risk profiles of new molecular entities during their development. One of the critical components in the MID3 strategy is physiologically-based pharmacokinetic (PBPK) modeling, which is a mechanistic framework to quantitatively describe in vivo drug disposition profiles based on drug- and system-dependent parameters.[1–3] By integrating in vitro-to-in vivo extrapolation (IVIVE) with PBPK modeling, PBPK-IVIVE is widely applied to predict in vivo disposition profiles of drugs in various clinical studies, such as drug-drug, drug-disease, and drug-gene interactions, that have not been tested yet. For the prediction of drug-drug interactions (DDIs), regulatory authorities in general have accepted the model outcomes on DDIs involving drug-metabolizing enzymes, particularly CYPs, whereas the predictive performance of transporter-mediated DDIs has not reached sufficient levels of confidence yet.[1–3] One of the reasons for the latter is that the interpretation of clinical significance of transporter-mediated DDIs is typically more complicated than that of drug-metabolizing enzyme-mediated DDIs. In addition, there are knowledge gaps that limit the confidence of DDI predictions to model transporter kinetics with appropriate drug exposures at the site of action.[3,4]

One of the adenosine triphosphate-binding cassette-transporters, ABCB1 (P-glycoprotein [Pgp]), has been extensively studied.[5–7] It has been recognized widely that Pgp plays a critical role for a variety of drugs in affecting the rate and extent of their absorption. Despite recently increased understanding of the role of Pgp in pharmacokinetics, it is still challenging to accurately predict the fraction of the dose absorbed (F_a) for Pgp substrates via PBPK modeling, largely due to several IVIVE factors, such as solubility/dissolution, permeability, and transporter kinetics. Consequently, it is difficult to quantitatively predict intestinal Pgp-mediated DDIs (Pgp-DDIs) from an IVIVE perspective for both substrates and inhibitors.[4,8,9] Knowledge gaps still remain in establishing an IVIVE for Pgp kinetics of both substrates (e.g., Michaelis-Menten constant [K_m] and maximal efflux rate [J_{max}]) and inhibitors (e.g., inhibition constant [K_i]). In fact, the US Food and Drug Administration (FDA) indicates in their reviews that there is uncertainty in quantitatively translating Pgp K_i values from in vitro to in vivo in the PBPK approach.[10]

In this study, we have investigated an IVIVE for Pgp-DDIs via PBPK modeling. We selected three Pgp substrates, digoxin, dabigatran etexilate, and quinidine, and two Pgp inhibitors, itraconazole and verapamil. Digoxin is largely excreted into urine as the unchanged drug whereas quinidine is mainly metabolized by CYP3A in liver with a moderate excretion into urine.[11,12] Quinidine also inhibits CYP2D6, CYP3A, and Pgp.[13,14] Dabigatran etexilate is a prodrug that is metabolized extensively by carboxylesterases to the pharmacologically active moiety, dabigatran, which is not a Pgp substrate.[15,16] Digoxin is categorized as class 3 in the Biopharmaceutics Classification System (BCS) whereas dabigatran etexilate and quinidine are BCS

class 1 drugs.[17] These Pgp substrates are hence considered soluble at clinical doses. We have previously developed and verified the PBPK models of digoxin, dabigatran etexilate, and quinidine to adequately describe rifampin-mediated DDIs due to intestinal Pgp induction.[18]

Regarding Pgp inhibitors used in this study, itraconazole and verapamil not only inhibit Pgp but also inhibit CYP3A.[8,19,20] In addition, the primary metabolites of itraconazole and verapamil, hydroxyitraconazole and norverapamil, respectively, also inhibit both Pgp and CYP3A.[21,22] PBPK models of itraconazole and hydroxyitraconazole have mainly been reported as CYP3A inhibitors, whereas one reported PBPK model included Pgp inhibition to predict the DDI with digoxin.[23–26] The Pgp K_i value used for this model was 0.008 μM for itraconazole without inputs for hydroxyitraconazole. PBPK models for verapamil and norverapamil were reported to account for the effects of both Pgp and CYP3A inhibition on DDIs with digoxin and midazolam, respectively.[20] Subsequently, the vendor-verified verapamil and norverapamil models from Simcyp (Certara UK Ltd., Simcyp Division, Sheffield, UK) have been applied to the DDI prediction with bosutinib, dabigatran etexilate, and rivaroxaban with or without modifications.[27–30] Pgp K_i values used in these models were 0.10 to 0.16 μM for verapamil and 0.04 to 0.3 μM for norverapamil, whereas PBPK models often utilized the lower end of the reported in vitro K_i values as the worst-case scenario. Overall, in these reports, only one Pgp substrate was used for the model verification and/or application, resulting in no comparisons of the predictive model performance among the different Pgp substrates. Furthermore, different K_i values of Pgp inhibitors have been used for DDI prediction with or without their metabolites. In the present study, we have therefore evaluated the predictive model performance of PBPK-IVIVE on clinical DDI studies between these substrates and inhibitors.

METHODS

PBPK modeling outline

A commercially available dynamic PBPK model, Simcyp population-based simulator (version 19.1), was used to simulate pharmacokinetics of the Pgp substrates and inhibitors. The advanced dissolution, absorption, and metabolism (ADAM) model implemented in Simcyp was utilized to predict F_a and a fraction of the dose escaping intestinal first-pass metabolism (F_g). Simulation of all clinical trials was performed with a virtual default population of 100 healthy volunteers in 10 trials of 10 subjects, each aged 20 to 50 years with a female/male ratio of 0.5. Clinical trial designs in the simulations were primarily set as the study design reported in the literature described below.

PBPK model input parameters

Input parameters of Pgp inhibitors and substrates in the PBPK models are summarized in Appendix S1. For Pgp inhibitors, compound files of itraconazole and hydroxyitraconazole were obtained from the literature whereas those of verapamil and norverapamil were from the Simcyp library.[25] These files were modified, such as Pgp K_i inputs in the ADAM model, and then verified based on the clinical results, as described in Appendix S1. In vitro half maximal inhibitory concentration (IC_{50}) for Pgp inhibition by itraconazole, hydroxyitraconazole, verapamil, and norverapamil against digoxin in Caco-2 cell monolayers were obtained from the database in Drug Interaction Solutions (DIDB database; University of Washington, Seattle, WA). Assuming K_i was half of the IC_{50} (to be conservative), K_i values used for PBPK modeling were 1.0 μM for itraconazole, 0.8 μM for hydroxyitraconazole, 2.0 μM for verapamil, 0.15 μM for norverapamil, and 0.8 μM for quinidine, as described in Appendix S1. In addition, itraconazole K_i value of 0.22 μM toward dabigatran etexilate in Caco-2 cell monolayers was also explored in the DDI prediction between itraconazole and dabigatran etexilate.

For Pgp substrates, the previously developed compound files of digoxin, dabigatran etexilate, dabigatran, and quinidine were primarily used in the present study.[18] In vitro Pgp kinetic parameters, K_m and J_{max}, were, respectively, 25 μM and 128 pmol/min/cm^2 for digoxin, 2.6 μM and 25 pmol/min/cm^2 for dabigatran etexilate and 1.0 μM and 21 pmol/min/cm^2 for quinidine. To adequately recover the plasma concentration-time profiles of the Pgp substrates in the control groups of each DDI study, the in vitro-to-in vivo Pgp scaling factors (Pgp-SFs) for J_{max} were optimized by the sensitivity analysis for the ratios of transporter activity or abundance in intestine between in vivo and in vitro (relative activity/expression factors, RAF/REF, in Simcyp). In contrast, the unbound K_m estimates in vitro were assumed to represent in vivo affinity (i.e., intrinsic values) as the general hypothesis. The refined compound files were then applied to the DDI prediction in the test groups with Pgp inhibitors.

PBPK modeling for DDI prediction

The DDI results of itraconazole and verapamil with digoxin, dabigatran etexilate, and quinidine were obtained from the literature as described in Appendix S1. A brief outline of the DDI studies is as follows:

- Itraconazole 200 mg once-daily with digoxin 0.5 mg ($n = 10$).[31]
- Itraconazole 200 mg once-daily with dabigatran etexilate 0.375 mg ($n = 8$).[21]
- Itraconazole 100 or 200 mg once-daily with quinidine sulfate 100 or 200 mg ($n = 6$ or 9).[12,32]
- Verapamil 80 mg three-times-daily with digoxin 0.25 mg ($n = 10$).[33]
- Verapamil 120 mg twice- or four-times-daily with dabigatran etexilate 150 mg ($n = 20$).[34]
- Verapamil 80 or 120 mg three-times-daily with quinidine sulfate 400 mg ($n = 6$).[35]

As indicated in Appendix S1, the PBPK modeling for the DDIs with verapamil and digoxin was performed at digoxin doses of 0.25 and 1 mg because plasma concentrations of digoxin in the control group of this study were approximately fourfold higher than the mean values from the meta-analysis of six studies following the dose-normalization. In the verapamil DDI study with dabigatran etexilate, total dabigatran (unconjugated and conjugated) concentrations were measured, whereas conjugated dabigatran, mainly glucuronides, was approximately 20% of total dabigatran based on the assay results before and after alkaline cleavage. Assuming that the differences were within variability deriving from various factors, such as the differences in subjects, studies, and bioanalytical assays, the reported values were used in the present study. This assumption was also made in the previous report based on the meta-analysis.[18]

Data analysis

Pharmacokinetic parameters of Pgp substrates, such as the maximal plasma concentrations (C_{max}) and the area under the plasma concentration-time curves (AUC), were obtained from the literature. When these parameters were not reported, the values were calculated from the reported clearance values with doses or the digitalized plasma concentration-time profiles by DigitizeIt version 2.3.3 (Bormann, Germany). Pharmacokinetic parameters, such as C_{max}, AUC, and the ratios of C_{max} (C_{max}R) and AUC (AUCR) in the test groups to the control groups are presented as either arithmetic mean, median, or geometric mean with standard deviations (SDs), 90% or 95% confidence intervals (CIs), or percent coefficients of variation (CV%) according to the literature. To estimate substrate Pgp-SFs, the local sensitivity analysis tool implemented in Simcyp were performed to assess the appropriate values. The simulations with the obtained Pgp-SF were thereafter performed with a virtual default population of 100 healthy volunteers in 10 trials of 10 subjects. The study conditions for the sensitivity analyses and the following simulations were based on the reported clinical study designs. To evaluate predictive model performance, the deviation of predicted from observed values was calculated as prediction error (PE):

$$\text{PE}\% = \frac{\text{Predicted value} - \text{Observed value}}{\text{Observed value}} \times 100$$

PE of less than or equal to ±25% was provisionally used as the predefined criteria for the model verification.[36,37]

RESULTS

Itraconazole DDIs with Pgp substrates

Clinically observed and PBPK model-predicted plasma concentration-time profiles of digoxin, dabigatran, and quinidine in the itraconazole DDI studies are presented in Figure 1. In the DDI study with digoxin, Pgp-SF for digoxin was estimated at 0.75 in the control group with PE of ±4% for C_{max} and AUC (Table 1). PBPK modeling sufficiently predicted the observed C_{max}R with PE of −11%, whereas AUCR was slightly underpredicted with PE of −27%. The predicted F_a in the control and test groups were ~0.8 and ~0.9, respectively. It is noteworthy that the predicted C_{max}R (1.20 ± 0.10) and AUCR (1.11 ± 0.07) were within the regulatory agency's criteria of negligible DDIs (±25%) whereas the observed ratios (1.34 and 1.52, respectively) were above the criteria. This could be the potential limitation on the use of PE% as the predictive model performance; therefore, we should carefully account for the variability in the predicted results (e.g., SDs and CIs) for making decisions.

In the DDI study with dabigatran etexilate, Pgp-SF for dabigatran etexilate was estimated at 90 in the control group with PE of −15% for C_{max} and 30% for AUC (Table 1). Using itraconazole in vitro K_i of 1 μM (against digoxin), PBPK modeling slightly underpredicted the observed C_{max}R and AUCR in the test group with PE of −30% to −50% (Table 1 and Figure 1). The predicted F_a increased from ~0.1 to ~0.3. In contrast, using in vitro K_i of 0.22 μM (against dabigatran etexilate), the modeling results showed PE of 32% for C_{max}R and −4% for AUCR. The predicted F_a in the control and test groups were ~0.1 and ~0.5, respectively.

In the DDI study of quinidine sulfate (100 mg) with itraconazole, Pgp-SF for quinidine was estimated at five in the control group with PE of ±8% for C_{max} and AUC (Table 1). PBPK modeling adequately predicted the observed C_{max}R and AUCR with PE of ±18% (Table 1 and

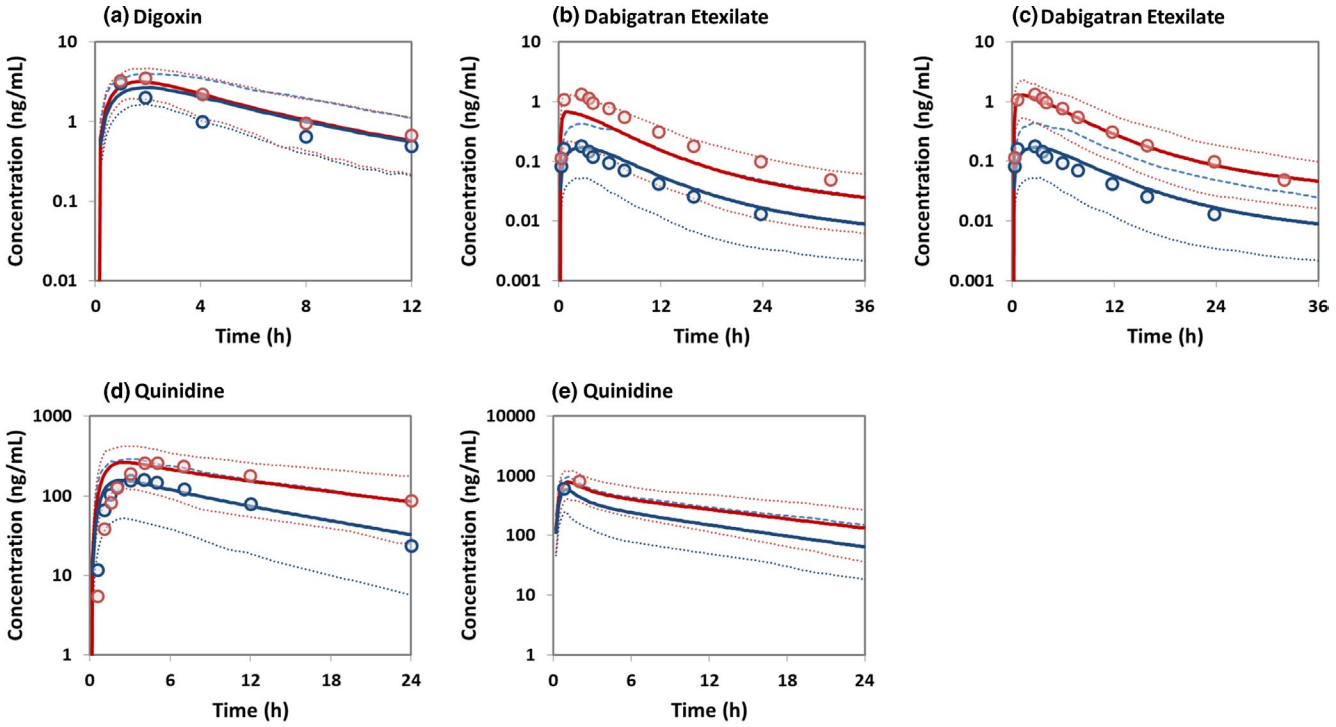

FIGURE 1 PBPK model-predicted and clinically observed plasma concentrations of digoxin, dabigatran, and quinidine in healthy subjects following a single oral administration with and without multiple-dose oral coadministration of itraconazole. Oral doses were digoxin 0.5 mg (a), dabigatran etexilate 0.375 mg (b, c), quinidine sulfate 100 mg (d), and 200 mg (e) with and without itraconazole 200 mg once-daily except for 100 mg once-daily (e). Itraconazole Pgp K_i values used were 1 μM (a, b, d, e) and 0.22 μM (c). The observed and predicted plasma concentration-time profiles were expressed as mean (circles) and mean (solid lines) with 5th and 95th percentiles (dotted line), respectively, in the control (blue) and test (red) groups, except for only the observed C_{max} (e). C_{max}, maximal plasma concentration; K_i, inhibition constant; PBPK, physiologically-based pharmacokinetic

Figure 1). The predicted F_a in the control and test groups were ~0.4 and ~0.5, respectively, while the predicted F_g was near-unity in both the groups. In another DDI study of quinidine sulfate (200 mg) with itraconazole, quinidine Pgp-SF was estimated at nine in the control group with PE of ±6% for C_{max} and AUC (Table 1). PEs for C_{max}R and AUCR in the test group were within ±25%. The predicted F_a was ~0.5 in the control group and ~0.6 in the test group, whereas the predicted F_g was near-unity in both the groups.

Overall, these results indicated that the PBPK-IVIVE for itraconazole reasonably described the clinical DDI results with digoxin, dabigatran etexilate, and quinidine.

Verapamil DDIs with Pgp substrates

Clinically observed and PBPK model-predicted plasma concentration-time profiles of digoxin, dabigatran, and quinidine in the verapamil DDI studies are presented in Figure 2. In the DDI study with digoxin, Pgp-SF for digoxin was estimated at 2.5 in the control group with PE of −16% for both C_{max} and AUC. In this study, PBPK modeling was performed at digoxin doses of 0.25 and 1 mg, as indicated above. The predicted C_{max}R and AUCR were comparable between the two doses (i.e., 1.59 vs. 1.61 and 1.41 vs. 1.44, respectively). The predicted C_{max}R and AUCR were also consistent with the observed results (1.44 and 1.50, respectively) with PE of ±12% (Table 2). The predicted F_a in the control and test groups were ~0.6 and ~0.7, respectively.

In the DDI study with dabigatran etexilate, Pgp-SF for dabigatran etexilate was estimated at 70 in the control group with PE of −17% for C_{max} and 13% for AUC (Table 2). PBPK modeling sufficiently predicted the observed C_{max}R and AUCR in three test groups following the different dosing regimens with PE of ±22%. The predicted F_a in the control group was 0.10, which increased to 0.12 to 0.15 in the test groups.

In the DDI study of quinidine sulfate with verapamil (80 and 120 mg three-times-daily), Pgp-SF for quinidine was estimated at two in the control group with PE of ±5% for C_{max} and AUC (Table 2). PBPK modeling sufficiently predicted the observed C_{max}R and AUCR in two test groups following the different dosing regimens with PE of ±18%. The predicted F_a and F_g were, respectively, 0.89 and 0.98 in the control group and 0.91 and 1.0 in the test group.

TABLE 1 PBPK model-predicted and clinically observed pharmacokinetic parameters of digoxin, quinidine, and dabigatran in DDI studies with itraconazole

Substrate	Group	Analysis	C_{max} (ng/ml)	AUC (ng·h/ml)	$C_{max}R$	AUCR
Digoxin 0.5 mg p.o.	Control	Obs	2.7 ± 1.6	23 ± 6	–	–
		Pred	2.7 ± 0.9	24 ± 9	–	–
		PE%	0	4	–	–
	Itraconazole 200 mg p.o. q.d.	Obs	3.7 ± 1.3	34 ± 6	1.34	1.52
		Pred	3.2± 0.9	26 ± 9	1.20 ± 0.10	1.11 ± 0.07
		PE%	−12	−25	−11	−27
Dabigatran Etexilate 0.375 mg p.o.	Control	Obs	0.17 (0.13 – 0.23)	1.4 (1.0 – 2.0)	–	–
		Pred	0.15 (0.13 – 0.16)	1.9 (1.4 – 2.3)	–	–
		PE%	−15	30	–	–
	Itraconazole 200 mg p.o. q.d.	Obs	1.1 (0.85 – 1.5)	10 (7.5 – 13)	6.4	6.9
		Pred[a]	0.62 (0.57 – 0.68)	6.3 (5.2 – 7.4)	4.3 (4.1 – 4.4)	3.4 (3.2 – 3.6)
		PE%	−43	−37	−34	−51
		Pred[b]	1.2 (1.2 – 1.3)	12 (11 – 14)	8.5 (8.0 – 9.0)	6.6 (6.0 – 7.3)
		PE%	13	24	32	−4
Quinidine 100 mg p.o.[c]	Control	Obs	174 ± 59	1980 ± 760	–	–
		Pred	160 ± 80	1921 ± 1010	–	–
		PE%	−8	−3	–	–
	Itraconazole 200 mg p.o. q.d.	Obs	276 ± 112	3890 ± 1460	1.59	1.96
		Pred	269 ± 95	3745 ± 1467	1.87 ± 0.49	2.14 ± 0.51
		PE%	−2	−4	18	9
Quinidine 200 mg p.o.[c]	Control	Obs	616 (487 – 1298)	5348 (4363 – 9211)	–	–
		Pred	635 (513 – 595)	5041 (4372 – 5255)	–	–
		PE%	3	−6	–	–
	Itraconazole 100 mg p.o. q.d.	Obs	811 (519 – 1038)	13817 (8290 – 19057)	1.32	2.58
		Pred	817 (725 – 811)	9622 (8562 – 10058)	1.39 (1.36 – 1.42)	1.94 (1.89 – 1.98)
		PE%	1	−30	5	−25

Note: Values are expressed as mean ± SD, median (95% confidence interval) or geometric mean (90% confidence interval).

Abbreviations: –, not reported or available; AUC, area-under the plasma concentration-time curve; AUCR, area-under the plasma concentration-time curve ratio; C_{max}, maximal plasma concentration; $C_{max}R$, maximal plasma concentration ratio; DDI, drug-drug interaction; K_i, inhibition constant; Obs, observed; PBPK, physiologically-based pharmacokinetic; PE, prediction error (%); Pred, predicted.

[a]Itraconazole Pgp K_i (1.0 μM) for digoxin as substrate.

[b]Itraconazole Pgp K_i (0.22 μM) for dabigatran etexilate as substrate.

[c]Quinidine sulfate doses (100 − 200 mg = 83 − 166 mg equivalents).

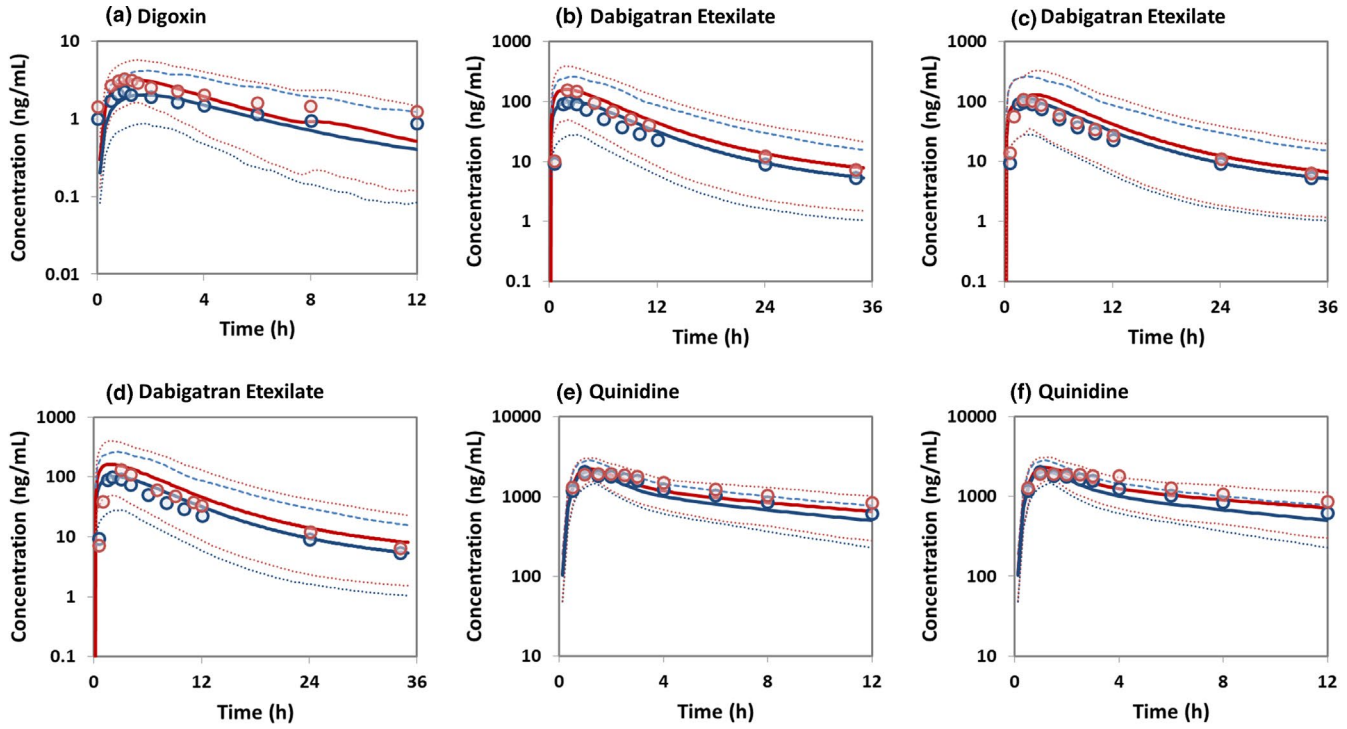

FIGURE 2 PBPK model-predicted and clinically observed plasma concentrations of digoxin, dabigatran, and quinidine in healthy subjects following a single oral administration with and without multiple-dose oral administration of verapamil. Oral doses were digoxin 0.25 mg (prediction at 1 mg) with verapamil 80 mg three-times-daily (a), dabigatran etexilate 150 mg 1 h after (b) or 2 h before (c) verapamil 120 mg twice-a-day or 1 h after verapamil 120 mg four-times-daily (d), quinidine sulfate 400 mg with verapamil 80 mg three-times-daily (e), or 120 mg three-times-daily (f). The observed and predicted plasma concentration-time profiles were expressed as mean (circles) and mean (solid lines) with 5th and 95th percentiles (dotted line), respectively, in the control (blue) and test (red) groups. PBPK, physiologically-based pharmacokinetic

Overall, these results indicated that the PBPK-IVIVE for verapamil reasonably described the clinical DDI results with digoxin, dabigatran etexilate, and quinidine.

Sensitivity analyses for substrate Pgp-SF and inhibitor K_i

The sensitivity analyses for the substrate Pgp-SF and the inhibitor Pgp K_i were performed to investigate the impacts of these parameters on the substrate F_a in the DDI studies. As presented in Figure 3, the predicted F_a for the substrates would significantly decline with the increases in the substrate Pgp-SFs (i.e., the increases in Pgp J_{max}) when the inhibitor K_i were relatively less potent (e.g., ≥0.1 μM). Similarly, the predicted substrate F_a would decline with the increases in the inhibitor K_i when the substrate Pgp-SFs were relatively higher (e.g., ≥5). In contrast, when either substrate Pgp-SF or inhibitor K_i was lower (e.g., ≤4 and ≤0.06 μM, respectively), the predicted F_a was less sensitive to these parameters. The lower Pgp-SF would readily cause saturation of Pgp activity whereas the lower (or more potent) inhibitor K_i could potentially lead to near-complete Pgp inhibition; thus, both the cases would result in higher F_a (e.g., ≥0.7). Overall, the modeling results suggested that both the substrate Pgp-SF and the inhibitor K_i would be key for prediction and/or understanding of Pgp-DDIs.

DISCUSSION

In the PBPK-IVIVE for clinical Pgp-DDIs, we first focused on the model verification of three Pgp substrates, digoxin, dabigatran etexilate, and quinidine, with Pgp-SF for J_{max}. This is based on the general hypothesis that unbound K_m for enzymes and transporters is intrinsic. The modeling results suggest that the optimization of substrate Pgp-SF is critical to adequately recover the clinical results. We then applied the PBPK models of two Pgp inhibitors, itraconazole and verapamil, with the in vitro Pgp K_i values to recover the clinical Pgp-DDIs with the Pgp substrates. The results suggest that the PBPK-IVIVE could adequately recover the Pgp-DDI results between these substates and inhibitors. Thus, the present PBPK-IVIVE approach appears to be successful in describing clinical Pgp-DDIs. However, the results clearly underscore the current challenges

TABLE 2 PBPK model-predicted and clinically observed pharmacokinetic parameters of digoxin, dabigatran, and quinidine in DDI studies with verapamil

Substrate	Group	Analysis	C_{max} (ng/ml)	AUC (ng·h/ml)	$C_{max}R$	AUCR
Digoxin 0.25 mg p.o.[a]	Control	Obs	2.5 ± 0.7	16 ± 2	–	–
		Pred	2.1 ± 1.1	13 ± 9	–	–
		PE%	−16	−16	–	–
	Verapamil 80 mg p.o. t.i.d.	Obs	3.6 ± 0.8	24 ± 3	1.44	1.50
		Pred	3.3 ± 1.5	18 ± 11	1.61 ± 0.21	1.44 ± 0.15
		PE%	−9	−22	12	−4
Dabigatran Etexilate 150 mg p.o.	Control	Obs	99 (75)	854 (62)	–	–
		Pred	83 (76)	964 (82)	–	–
		PE%	−17	13	–	–
	Verapamil 120 mg p.o. b.i.d. 1-h predose	Obs	162 (60)	1310 (55)	1.63 (1.22 – 2.17)	1.54 (1.19 – 1.99)
		Pred	133 (70)	1462 (74)	1.61 (1.58 – 1.64)	1.52 (1.49 – 1.54)
		PE%	−18	12	−1	−1
	Verapamil 120 mg p.o. b.i.d. 2-h postdose	Obs	111 (87)	1010 (75)	1.12 (0.84 – 1.49)	1.18 (0.91 – 1.52)
		Pred	106 (75)	1236 (80)	1.29 (1.26 – 1.32)	1.28 (1.26 – 1.30)
		PE%	−4	22	15	8
	Verapamil 120 mg p.o. q.i.d. 1-h predose	Obs	132 (86)	1190 (74)	1.34 (1.00 – 1.80)	1.39 (1.07 – 1.81)
		Pred	135 (70)	1499 (74)	1.64 (1.60 – 1.67)	1.56 (1.53 – 1.58)
		PE%	2	26	22	12
Quinidine 400 mg p.o.[b]	Control	Obs	2047	19529 ± 4710	–	–
		Pred	2106 ± 429	18546 ± 6722	–	–
		PE%	3	−5	–	–
	Verapamil 80 mg p.o. t.i.d.	Obs	1957	28621 ± 5675	0.96	1.47
		Pred	2291 ± 473	24944 ± 9811	1.09 ± 0.03	1.33 ± 0.15
		PE%	18	−13	14	−9
	Verapamil 120 mg p.o. t.i.d.	Obs	1939	29381 ± 6500	0.95	1.50
		Pred	2353 ± 485	28140 ± 11072	1.12 ± 0.04	1.51 ± 0.24
		PE%	21	−4	18	0

Note: Values are expressed as mean, mean ± SD or geometric mean (coefficient of variation%).

Abbreviations: –, not reported or available; AUC, area-under the plasma concentration-time curve; AUCR, area-under the plasma concentration-time curve ratio; C_{max}, maximal plasma concentration; $C_{max}R$, maximal plasma concentration ratio; DDI, drug-drug interaction; Obs, observed; PBPK, physiologically-based pharmacokinetic; PE, prediction error (%); Pred, predicted.

[a]Prediction was performed at 1 mg.

[b]Quinidine sulfate doses (400 mg = 332 mg equivalents).

on PBPK-IVIVE on Pgp-DDIs. Some potential issues are identified and warrant further investigation and discussion.

One of the main challenges on the Pgp-DDI prediction associated with PBPK-IVIVE is to accurately determine substrate Pgp kinetics in vitro (K_m and J_{max})

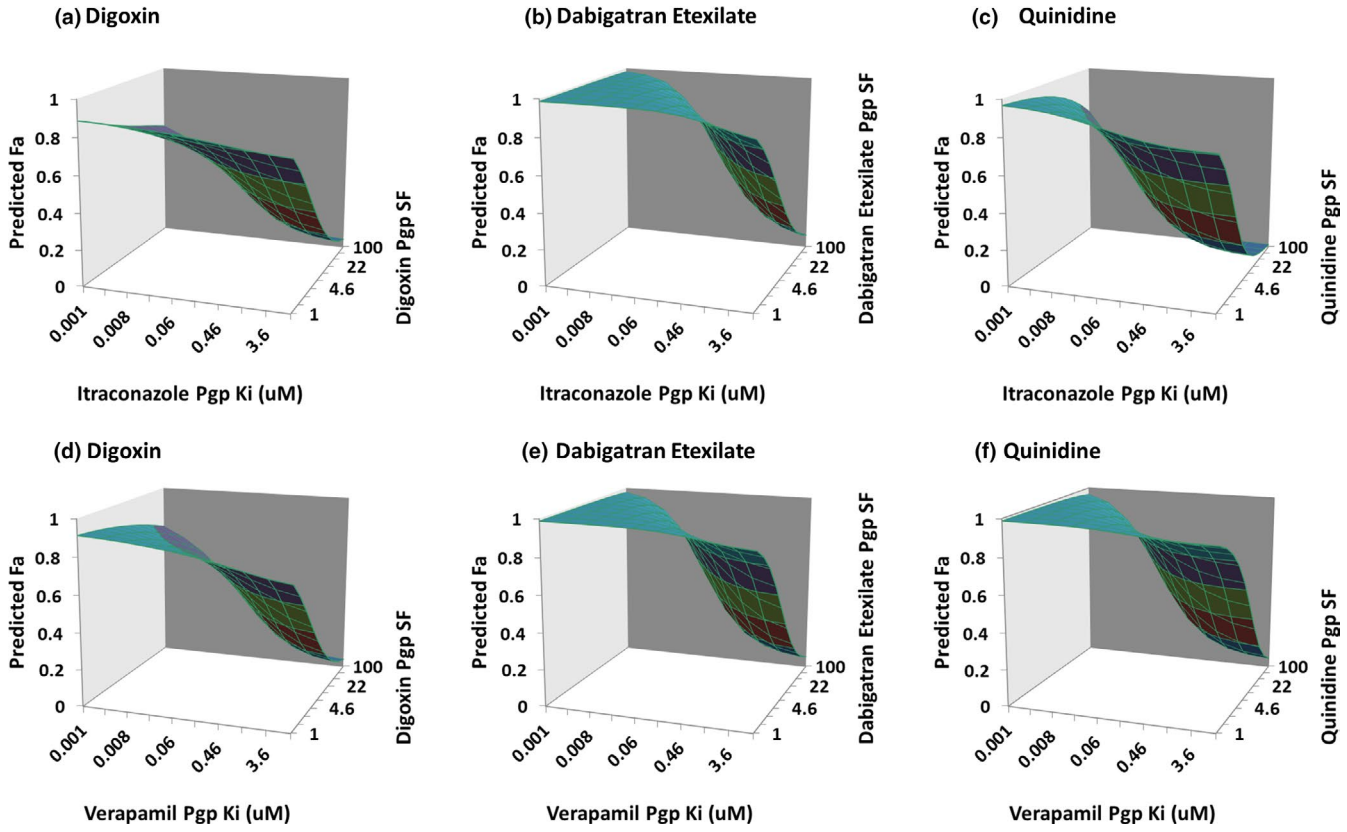

FIGURE 3 The relationships among the PBPK model-predicted Pgp substrate F_a, intestinal Pgp J_{max} scaling factor (Pgp-SF), and Pgp inhibitor K_i in healthy subjects following a single oral administration of Pgp substrates with multiple-dose oral coadministration of itraconazole or verapamil. Oral doses were digoxin 0.5 mg (a), dabigatran etexilate 0.375 mg (b), quinidine sulfate 100 mg (c), digoxin 1 mg (d), dabigatran etexilate 150 mg (e), and quinidine sulfate 400 mg (f) with itraconazole 200 mg once-daily (a, b, c) or verapamil 80 mg three-times-daily (d), 120 mg twice-daily (e), and 120 mg three-times-daily (f). The ranges of Pgp-SF were 1 to 100 against the Pgp inhibitor K_i of 0.001 to 10 μM. F_a, fraction of the dose absorbed; J_{max}, maximal efflux rate; K_i, inhibition constant; PBPK, physiologically-based pharmacokinetic

because of a large inter-laboratory variability associated with various factors such as different cell lines and transporter kinetic equations/models.[4,38] The current strategy to overcome these limitations is to adequately model in vitro data, where transporter kinetics with unbound substrate concentrations at the binding site can be taken into account along with flux through two diffusional barriers.[4,38] We used the previously reported Pgp kinetic parameters, which were determined by fitting in vitro Caco-2 data (from a laboratory) to the compartmental model.[18] In the compartment model used, K_m is defined as an intracellular unbound concentration and governed by the substrate-Pgp interaction, yielding independent K_m estimates from Pgp expression levels.[39] In vitro unbound K_m estimates are thus assumed to represent in vivo affinity (i.e., intrinsic values). In contrast, Pgp-SFs for J_{max} could account for the differences in Pgp expression or functional activity between in vitro and in vivo, although this might be drug-dependent due to some other factors, such as the regional difference of Pgp abundance along the various regions of intestine and drug absorption sites.[40,41] Accordingly, we have estimated substrate Pgp-SFs to adequately recover the observed results of control groups in each study, given an expected variability derived from various factors such as intra- and intersubjects and studies.

Similarly, in vitro Pgp K_i values have been reported to show a large variability among laboratories due to multiple factors, including different substrates and cell lines with various Pgp expression levels.[9,42] For instance, the in vitro K_i values for digoxin varied from 20 to 800-fold for 15 Pgp inhibitors among 22 laboratories.[43,44] In the present study, we primarily used the median K_i values of Pgp inhibitors against digoxin in Caco-2 cell monolayers obtained from the DIDB database. The Pgp IC_{50} values varied considerably from 0.46 to 6.0 μM (median 2.0 μM) for itraconazole and 0.06 to 17 μM (4.0 μM) for verapamil. Median IC_{50} value for itraconazole against dabigatran etexilate in Caco-2 cell monolayers (0.44 μM) was ~5-folder lower than that against digoxin (2 μM). In the Pgp-DDI prediction between itraconazole and dabigatran etexilate, the PE for C_{max}R and AUCR were −34% and

−51%, respectively, when using the K_i value for digoxin whereas those were 32% and −4%, respectively, when using the K_i value for dabigatran etexilate (Table 1). The sensitivity analysis revealed that itraconazole Pgp K_i of ~0.3 μM yielded a reasonable prediction with PE of ±16% for C_{max}R and AUCR, suggesting that itraconazole K_i in the best fit was relatively closer to that for dabigatran etexilate relative to digoxin. This suggests that it is important to determine in vitro K_i toward appropriate Pgp substrates, which can be supported with the reasonable prediction of verapamil DDIs with digoxin and quinidine because of comparable verapamil IC_{50} between digoxin (4.0 μM) and quinidine (3.9 μM). We could not further investigate this point because in vitro K_i values for itraconazole and verapamil against other Pgp substrate were limited in the DIDB database. Despite the reasonable Pgp-DDI prediction, one of the limitations of the present modeling is that the median IC_{50} values obtained from the DIDB database were used whereas the compartment modeling analyses for Pgp kinetic estimation have been recommended.[38,42] Therefore, this point should be addressed in the future, although, at this moment, the traditional extracellular concentration-based analyses for estimating Pgp IC_{50} is still widely used and in general accepted by regulatory agencies.[45-47] Another limitation is that inhibitors' K_i is incorporated into only intestine and/or liver to focus on Pgp-DDIs on absorption, including re-absorption via biliary excretion. As digoxin and quinidine are excreted into urine, there is a possibility for Pgp-mediated DDIs in the kidneys.[14,15] However, the modeling results exhibited that Pgp K_i values used in the present studies were at least several fold higher than steady-state unbound C_{max} of Pgp inhibitors; for instance, ~10-fold for itraconazole and 20-fold for hydroxyitraconazole following itraconazole 200 mg once-daily, and 40-fold for verapamil and 5-fold for norverapamil following verapamil 120 mg twice-daily. Therefore, systemic effects of Pgp inhibitors on Pgp-DDIs can be expected to be minimal unless a significant accumulation of unbound drugs takes place in certain tissues.

The model-predicted substrate F_a decreases with increases in Pgp-SFs for J_{max} when Pgp activity is neither saturated nor inhibited at given doses (Figure 3). Pgp-SFs used in this study ranged from 0.75 to 2.5 for digoxin at 0.25 to 1 mg, 70 to 90 for dabigatran etexilate at 0.375 to 150 mg, and 2 to 9 for quinidine sulfate at 100 to 400 mg, corresponding to the predicted F_a of 0.54 to 0.85, 0.06 to 0.14, and 0.41 to 0.93, respectively. Hence, the predicted F_a showed roughly two-fold difference among the studies, which could be conceivable given the different doses and study conditions along with expected variability. In addition, quinidine is known to exhibit supraproportional increases in oral exposures at the doses used in this study.[12,13,32,35] These differences potentially lead to different degrees of Pgp-DDIs depending on substrate F_a, as simulated in Figure 3. Therefore, it would be critical to optimize substrate Pgp-SF to sufficiently predict Pgp-DDIs, as the FDA guidance indicates that the sponsor should establish and verify PBPK models for transporter substrates before applying for DDI predictions.[45] The range of predicted F_a for digoxin (0.54 to 0.85) corresponds to the extent of increases in oral exposure by 1.2 to 2-fold when digoxin F_a increases up to unity due to a complete Pgp inhibition. The European Medicines Agency (EMA) guidance recommends that dabigatran etexilate is a better probe Pgp substrate for clinical DDI studies because of its lower F_a (~0.1).[46] In the clinical DDI studies used for the present study, the observed C_{max}R and AUCR for digoxin and quinidine were within two-fold with the exception of AUCR (~2.6-fold) in one of four DDI results with quinidine. In contrast, those for dabigatran were six to seven-fold at the microdose of dabigatran etexilate (0.375 mg) with itraconazole and ~1.5-fold at the clinically recommended dose of dabigatran etexilate (150 mg) with verapamil. This may suggest that the microdose of dabigatran etexilate is more sensitive for clinical Pgp-DDI studies, which can also be reasonably predicted by the present PBPK-IVIVE.

In the itraconazole and verapamil PBPK models, Pgp K_i values for parent drugs were incorporated into intestine and liver whereas those for metabolites were only in liver. This is because the ADAM model is not available for inhibitor metabolites in Simcyp, resulting in metabolite-mediated intestinal Pgp inhibition being dynamically predicted by plasma concentrations in portal vein corrected for unbound fraction in enterocytes ($f_{u,gut}$), e.g., total plasma concentrations when $f_{u,gut}$ is unity. In both the compound files of hydroxyitraconazole from the literature and norverapamil from the Simcyp library, the input values of $f_{u,gut}$ are set at unity.[25] In contrast, unbound enterocyte concentrations predicted by the ADAM model are used for the prediction of parent drug-mediated intestinal Pgp inhibition. It is noteworthy that the predicted F_g for itraconazole and verapamil were ~1 and ~0.8, respectively, suggesting minimal metabolite formations in enterocytes. The present PBPK modeling therefore assumed that metabolite-mediated Pgp inhibition was negligible in the intestines, which will (and should) be investigated further. This also includes the distribution (rate and extent) of metabolites (and parent drug administered intravenously) from the portal vein to the lipid bilayer in the apical membrane of enterocytes where Pgp interacts with substrates and inhibitors via conformational changes coupling ATP hydrolysis.[48–50]

In summary, the present study has demonstrated that clinical Pgp-DDIs among three substrates and two inhibitors could be reasonably described by PBPK-IVIVE with

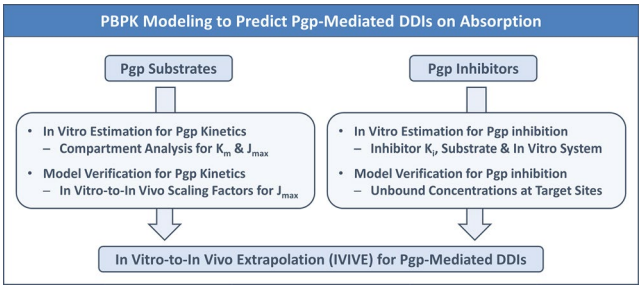

FIGURE 4 PBPK modeling scheme to predict Pgp-mediated DDIs between Pgp substrates and inhibitors. DDI, drug-drug interaction; J_{max}, maximal efflux rate; K_i, inhibition constant; K_m, Michaelis-Menten constant; PBPK, physiologically-based pharmacokinetic

Pgp kinetic parameters determined in vitro. The present modeling approach can be applicable to predict Pgp-DDIs with other Pgp substrates and inhibitors. In addition, the modeling results also suggest that Pgp kinetic parameters of both the substrates (K_m and J_{max}) and inhibitors (K_i) are key for successful DDI prediction because these parameters are sensitive to substrate F_a in Pgp-DDIs. It would also be critical to incorporate appropriate unbound inhibitor concentrations at the site of action into PBPK modeling. These points are graphically summarized in Figure 4 as the PBPK-IVIVE scheme for Pgp-DDI prediction, which is in line with the FDA guidance and the industry review.[4,45] The present results support a quantitative prediction of Pgp-DDIs using in vitro parameters, which will significantly increase the value of in vitro studies to design and run clinical DDI studies safely and effectively.

ACKNOWLEDGEMENT

The authors greatly acknowledge Sibylle Neuhoff (Certara UK Ltd., Simcyp Division, Sheffield, UK) for valuable inputs on PBPK modeling.

CONFLICT OF INTEREST

The authors are employees of Janssen Research & Development.

AUTHOR CONTRIBUTIONS

S.Y., R.E., and L.DZ. wrote the manuscript. S.Y. designed and performed the research and analyzed the data.

REFERENCES

1. Grimstein M, Yang Y, Zhang, X, et al. Physiologically based pharmacokinetic modeling in regulatory science: an update from the U.S. Food and Drug Administration's Office of Clinical Pharmacology. *J Pharm Sci*. 2019;108:21-25.
2. El-Khateeb E, Burkhill S, Murby S, et al. Physiological-based pharmacokinetic modeling trends in pharmaceutical drug development over the last 20-years; in-depth analysis of applications, organizations, and platforms. *Biopharm Drug Dispos*. 2021;42(4):107-117.
3. Shebley M, Sandhu P, Emami Riedmaier A, et al. Physiologically based pharmacokinetic model qualification and reporting procedures for regulatory submissions: a consortium perspective. *Clin Pharmacol Ther*. 2018;104:88-110.
4. Taskar KS, Pilla Reddy V, Burt H, et al. Physiologically-based pharmacokinetic models for evaluating membrane transporter mediated drug-drug interactions: current capabilities, case studies, future opportunities, and recommendations. *Clin Pharmacol Ther*. 2020;107:1082-1115.
5. Chen Z, Shi T, Zhang L, et al. Mammalian drug efflux transporters of the ATP binding cassette (ABC) family in multidrug resistance: A review of the past decade. *Cancer Lett*. 2016;370:153-164.
6. Ben Saad A, Bruneau A, Mareux E, et al. Molecular regulation of canalicular ABC transporters. *Int J Mol Sci*. 2021;22(4):2113.
7. Wolking S, Schaeffeler E, Lerche H, Schwab M, Nies AT. Impact of genetic polymorphisms of ABCB1 (MDR1, P-Glycoprotein) on drug disposition and potential clinical implications: update of the literature. *Clin Pharmacokinet*. 2015;54:709-735.
8. Fenner KS, Troutman MD, Kempshall S, et al. Drug-drug interactions mediated through P-glycoprotein: clinical relevance and in vitro-in vivo correlation using digoxin as a probe drug. *Clin Pharmacol Ther*. 2009;85:173-181.
9. Chaudhry A, Chung G, Lynn A, et al. Derivation of a system-independent Ki for P-glycoprotein mediated digoxin transport from system-dependent IC50 data. *Drug Metab Dispos*. 2018;46:279-290.
10. US Food and Drug Administration (FDA). Application Number: 212018Orig1s000, MULTI-DISCIPLINE REVIEW. https://www.accessdata.fda.gov/drugsatfda_docs/nda/2019/212018Orig1s000MultidisciplineR.pdf. Accessed April 1, 2021.
11. Iisalo E. Clinical pharmacokinetics of digoxin. *Clin Pharmacokinet*. 1977;2:1-16.
12. Damkier P, Hansen LL, Brøsen K. Effect of diclofenac, disulfiram, itraconazole, grapefruit juice and erythromycin on the pharmacokinetics of quinidine. *Br J Clin Pharmacol*. 1999;48:829-838.
13. Galetin A, Clarke SE, Houston JB. Quinidine and haloperidol as modifiers of CYP3A4 activity: multisite kinetic model approach. *Drug Metab Dispos*. 2002;30:1512-1522.
14. Kishimoto W, Ishiguro N, Ludwig-Schwellinger E, Ebner T, Maeda K, Sugiyama Y. Usefulness of a model-based approach for estimating in vitro P-glycoprotein inhibition potency in a transcellular transport assay. *J Pharm Sci*. 2016;105:891-896.
15. Blech S, Ebner T, Ludwig-Schwellinger E, Stangier J, Roth W. The metabolism and disposition of the oral direct thrombin inhibitor, dabigatran, in humans. *Drug Metab Dispos*. 2008;36:386-399.
16. Laizure SC, Parker RB, Herring VL, Hu ZY. Identification of carboxylesterase-dependent dabigatran etexilate hydrolysis. *Drug Metab Dispos*. 2014;42:201-206.
17. Benet LZ, Broccatelli F, Oprea TI. BDDCS applied to over 900 drugs. *AAPS J*. 2011;13:519-547.
18. Yamazaki S, Costales C, Lazzaro S, Eatemadpour S, Kimoto E, Varma MV. Physiologically-based pharmacokinetic modeling approach to predict rifampin-mediated intestinal P-glycoprotein induction. *CPT Pharmacometrics Syst Pharmacol*. 2019;8:634-642.

19. Zhang L, Zhang Y, Huang SM. Scientific and regulatory perspectives on metabolizing enzyme-transporter interplay and its role in drug interactions: challenges in predicting drug interactions. *Mol Pharm*. 2009;6:1766-1774.
20. Neuhoff S, Yeo KR, Barter Z, Jamei M, Turner DB, Rostami-Hodjegan A. Application of permeability-limited physiologically-based pharmacokinetic models: part II - prediction of P-glycoprotein mediated drug-drug interactions with digoxin. *J Pharm Sci*. 2013;102:3161-3173.
21. Prueksaritanont T, Tatosian D, Chu X, et al. Validation of a microdose probe drug cocktail for clinical drug interaction assessments for drug transporters and CYP3A. *Clin Pharmacol Ther*. 2017;101:519-530.
22. Pauli-Magnus C, van Richter O, Burk O, et al. Characterization of the major metabolites of verapamil as substrates and inhibitors of P-glycoprotein. *J Pharmacol Exp Ther*. 2000;293:376-382.
23. Chen Y, Ma F, Lu T, et al. Development of a physiologically based pharmacokinetic model for itraconazole pharmacokinetics and drug-drug interaction prediction. *Clin Pharmacokinet*. 2016;55:735-749.
24. Prieto Garcia L, Janzén D, Kanebratt KP, Ericsson H, Lennernäs H, Lundahl A. Physiologically based pharmacokinetic model of itraconazole and two of its metabolites to improve the predictions and the mechanistic understanding of CYP3A4 drug-drug interactions. *Drug Metab Dispos*. 2018;46:1420-1433.
25. Chen Y, Cabalu TD, Callegari E, et al. Recommendations for the design of clinical drug-drug interaction studies with itraconazole using a mechanistic physiologically-based pharmacokinetic model. *CPT Pharmacometrics Syst Pharmacol*. 2019;8:685-695.
26. Hanke N, Frechen S, Moj D, et al. PBPK models for CYP3A4 and P-gp DDI prediction: a modeling network of rifampicin, itraconazole, clarithromycin, midazolam, alfentanil and digoxin. *CPT Pharmacometrics Syst Pharmacol*. 2018;7:647-659.
27. Otsuka Y, Choules MP, Bonate PL, Komatsu K. Physiologically-based pharmacokinetic modeling for the prediction of a drug-drug interaction of combined effects on P-glycoprotein and cytochrome P450 3A. *CPT Pharmacometrics Syst Pharmacol*. 2020;9:659-669.
28. Doki K, Neuhoff S, Rostami-Hodjegan A, Homma M. Assessing potential drug-drug interactions between dabigatran etexilate and a P-glycoprotein inhibitor in renal impairment populations using physiologically based pharmacokinetic modeling. *CPT Pharmacometrics Syst Pharmacol*. 2019;8:118-126.
29. Farhan N, Cristofoletti R, Basu S, et al. Physiologically based pharmacokinetics modeling to investigate formulation factors influencing the generic substitution of dabigatran etexilate. *CPT Pharmacometrics Syst Pharmacol*. 2021;10(3):199-210.
30. Yamazaki S, Loi CM, Kimoto E, Costales C, Varma MV. Application of physiologically based pharmacokinetic modeling in understanding bosutinib drug-drug interactions: importance of intestinal P-glycoprotein. *Drug Metab Dispos*. 2018;46:1200-1211.
31. Jalava KM, Partanen J, Neuvonen PJ. Itraconazole decreases renal clearance of digoxin. *Ther Drug Monit*. 1997;19:609-613.
32. Kaukonen KM, Olkkola KT, Neuvonen PJ. Itraconazole increases plasma concentrations of quinidine. *Clin Pharmacol Ther*. 1997;62:510-517.
33. Rodin SM, Johnson BF, Wilson J, Ritchie P, Johnson J. Comparative effects of verapamil and isradipine on steady-state digoxin kinetics. *Clin Pharmacol Ther*. 1988;43:668-672.
34. Hartter S, Sennewald R, Nehmiz G, Reilly P. Oral bioavailability of dabigatran etexilate (Pradaxa((R))) after co-medication with verapamil in healthy subjects. *Br J Clin Pharmacol*. 2013;75:1053-1062.
35. Edwards DJ, Lavoie R, Beckman H, Blevins R, Rubenfire M. The effect of coadministration of verapamil on the pharmacokinetics and metabolism of quinidine. *Clin Pharmacol Ther*. 1987;41:68-73.
36. Yamazaki S. Relationships of changes in pharmacokinetic parameters of substrate drugs in drug-drug interactions on metabolizing enzymes and transporters. *J Clin Pharmacol*. 2018;58(8):1053-1060.
37. Guest EJ, Aarons L, Houston JB, Rostami-Hodjegan A, Galetin A. Critique of the two-fold measure of prediction success for ratios: application for the assessment of drug-drug interactions. *Drug Metab Dispos*. 2011;39:170-173.
38. Zamek-Gliszczynski MJ, Lee CA, Poirier A, et al. ITC recommendations for transporter kinetic parameter estimation and translational modeling of transport-mediated PK and DDIs in humans. *Clin Pharmacol Ther*. 2013;94:64-79.
39. Tachibana T, Kitamura S, Kato M, et al. Model analysis of the concentration-dependent permeability of P-gp substrates. *Pharm Res*. 2010;27:442-446.
40. Englund G, Rorsman F, Rönnblom A, et al. Regional levels of drug transporters along the human intestinal tract: co-expression of ABC and SLC transporters and comparison with Caco-2 cells. *Eur J Pharm Sci*. 2006;29:269-277.
41. Mouly S, Paine MF. P-glycoprotein increases from proximal to distal regions of human small intestine. *Pharm Res*. 2003;20:1595-1599.
42. Lee CA, Kalvass JC, Galetin A, Zamek-Gliszczynski MJ. ITC commentary on the prediction of digoxin clinical drug-drug interactions from in vitro transporter assays. *Clin Pharmacol Ther*. 2014;96:298-301.
43. Bentz J, O'Connor MP, Bednarczyk D, et al. Variability in P-glycoprotein inhibitory potency (IC50) using various in vitro experimental systems: implications for universal digoxin drug-drug interaction risk assessment decision criteria. *Drug Metab Dispos*. 2013;41:1347-1366.
44. Ellens H, Deng S, Coleman JA, et al. Application of receiver operating characteristic analysis to refine the prediction of potential digoxin drug interactions. *Drug Metab Dispos*. 2013;41:1367-1374.
45. US Food and Drug Administration (FDA). In Vitro Drug Interaction Studies — Cytochrome P450 Enzyme- and Transporter-Mediated Drug Interactions Guidance for Industry. https://www.fda.gov/media/134582/download. Accessed April 1, 2021.
46. European Medicines Agency (EMA). Guideline on the Investigation of Drug Interactions. http://www.ema.europa.eu/docs/en_GB/document_library/Scientific_guideline/2012/07/WC500129606.pdf. http://www.accessdata.fda.gov/drugsatfda_

docs/nda/2011/202570Orig1s000SumR.pdf. Accessed April 1, 2021.
47. Pharmaceuticals and Medical Devices Agency (PMDA). Guideline on drug interaction for drug development and appropriate provision of information. 2021. https://www.pmda.go.jp/files/000228122.pdf. Accessed April 1, 2021.
48. Clay AT, Sharom FJ. Lipid bilayer properties control membrane partitioning, binding, and transport of p-glycoprotein substrates. *Biochemistry*. 2013;52:343-354.
49. Loo TW, Bartlett MC, Clarke DM. Drug binding in human P-glycoprotein causes conformational changes in both nucleotide-binding domains. *J Biol Chem*. 2003;278:1575-1578.
50. Loo TW, Clarke DM. Recent progress in understanding the mechanism of P-glycoprotein-mediated drug efflux. *J Membr Biol*. 2005;206:173-185.

SUPPORTING INFORMATION

Additional supporting information may be found in the online version of the article at the publisher's website.

How to cite this article: Yamazaki S, Evers R, De Zwart L. Physiologically-based pharmacokinetic modeling to evaluate in vitro-to-in vivo extrapolation for intestinal P-glycoprotein inhibition. *CPT Pharmacometrics Syst Pharmacol*. 2022;11:55–67. doi:10.1002/psp4.12733